Supplementary Information

Low-energy catalytic methanolysis of poly(ethyleneterephthalate)

Duong Dinh Pham[a,b] and Joungmo Cho[a,b,*]

a. Research Centre for Green Carbon Catalysis, Korea Research Institute of Chemical Technology (KRICT), Daejeon, 34114, Republic of Korea

b. Department of Advanced Materials and Chemical Engineering, University of Science and Technology (UST), Daejeon, 34113, Republic of Korea

* Corresponding author information

Address: Research Centre for Green Carbon Catalysis, Korea Research Institute of Chemical Technology (KRICT), Daejeon, 34114, Republic of Korea

E-mail: jmcho@krict.re.kr / Phone: +82-42-860-7699 / Fax: +82-42-860-7388

S1. Methanolysis products from solvent-aided catalytic methanolysis

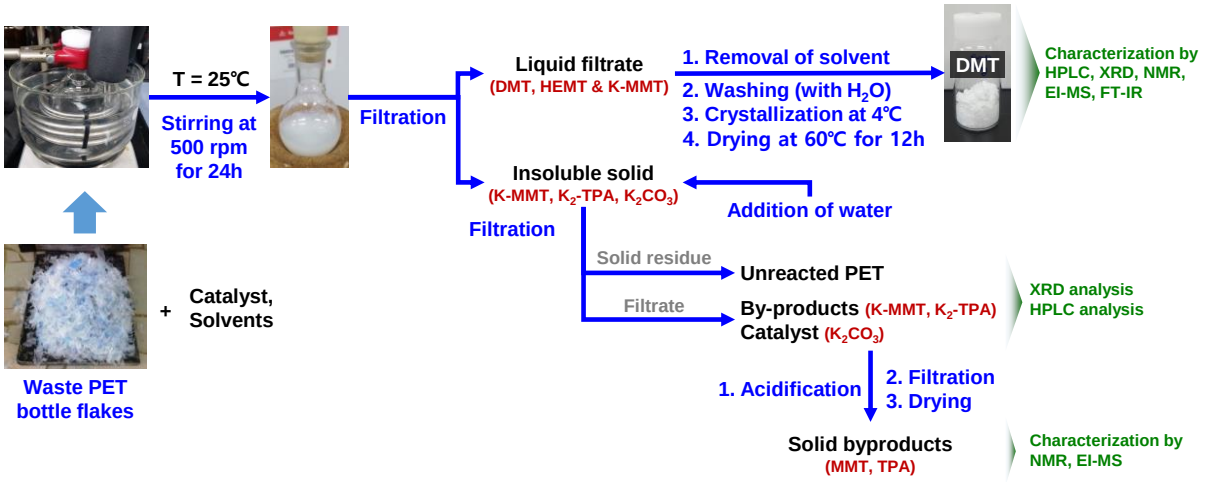

Fig. S1. Experimental procedure of solvent aided catalytic methanolysis of PET

A detailed experimental procedure for PET methanolysis is presented in Fig. S1. After 24 h reaction, the reaction mixture was filtered and separated into liquid mixture and insoluble solid residue. The liquid filtrate composed of dimethyl terephthalate (DMT), 2-hydroxyethyl methyl terephthalate (HEMT), and saturated potassium monomethyl terephthalate (K-MMT). The concentrations of DMT, HEMT and K-MMT were quantified by HPLC calibrated with standard materials. A rotary evaporator was used to remove all solvents from the mixture and then an excessive amount of distilled water was added. The resulting aqueous solution was transferred to the refrigerator (4°C) and kept there for 12 h. White-needle crystals were recovered from the mixture by filtration and dried in an air oven at 60 °C for 12 h. Dried sample were collected as a 'purified DMT' and characterized by ^{1}H-NMR, EI-MS, FT-IR and etc.

The insoluble solid contains unreacted PET, catalytic particles (K_2CO_3), potassium monomethyl terephthalic acid (K-MMT) and potassium terephthalate (K_2-TPA). The crystalline structure of solid samples was measured by a wide-angle x-ray diffraction. For each sample, two-step solvent dilutions (First, the sample was diluted with water at a ratio of 1:50 first. And then a small amount is taken and diluted in 70% (v/v) of methanol solutions at a ratio of 1:100) for by-products quantification by HPLC. By-products were crystallized by acid titration, followed by isolation (filtration and drying). Obtained by-products (TPA and MMT) were characterized by ^{1}H-NMR, EI-MS.

Fig. S2 and S3 presents the characterization results for DMT (methanolysis product) and solid residue containing by-products (TPA and MMT). For the structural analysis, EI-MS, NMR, HPLC and FT-IR were used.

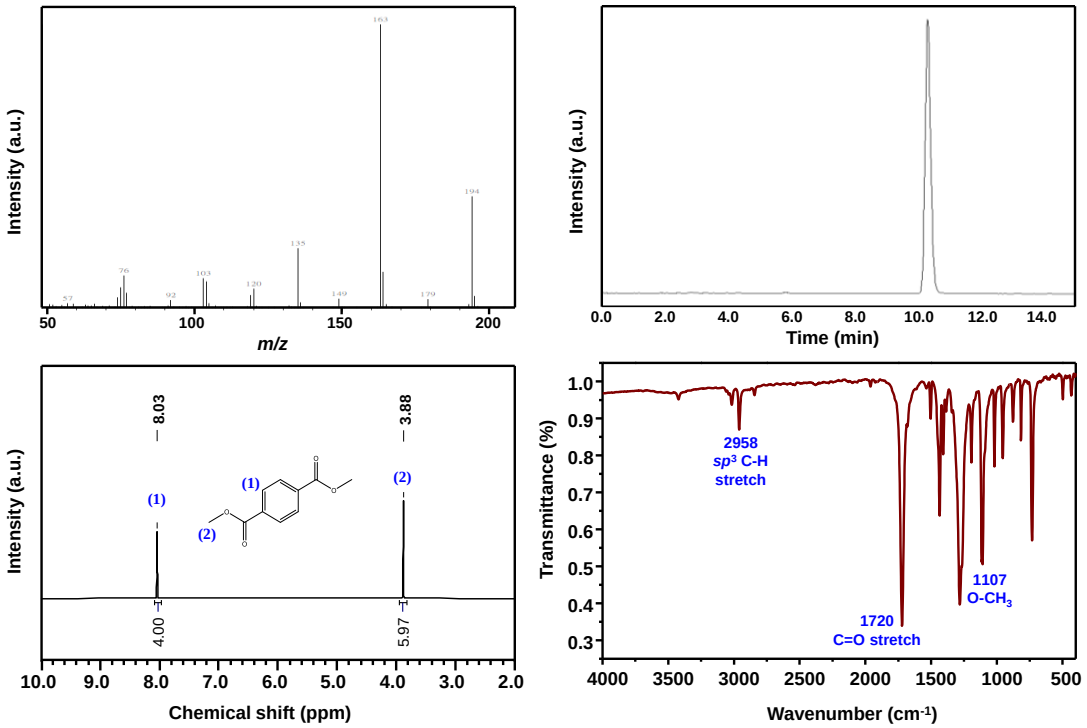

Fig. S2. (a) Fragmentation pattern by EI-MS, (b) HPLC chromatogram, (c) ^{1}H NMR spectrum, and (d) FT-IR spectrum of purified DMT.

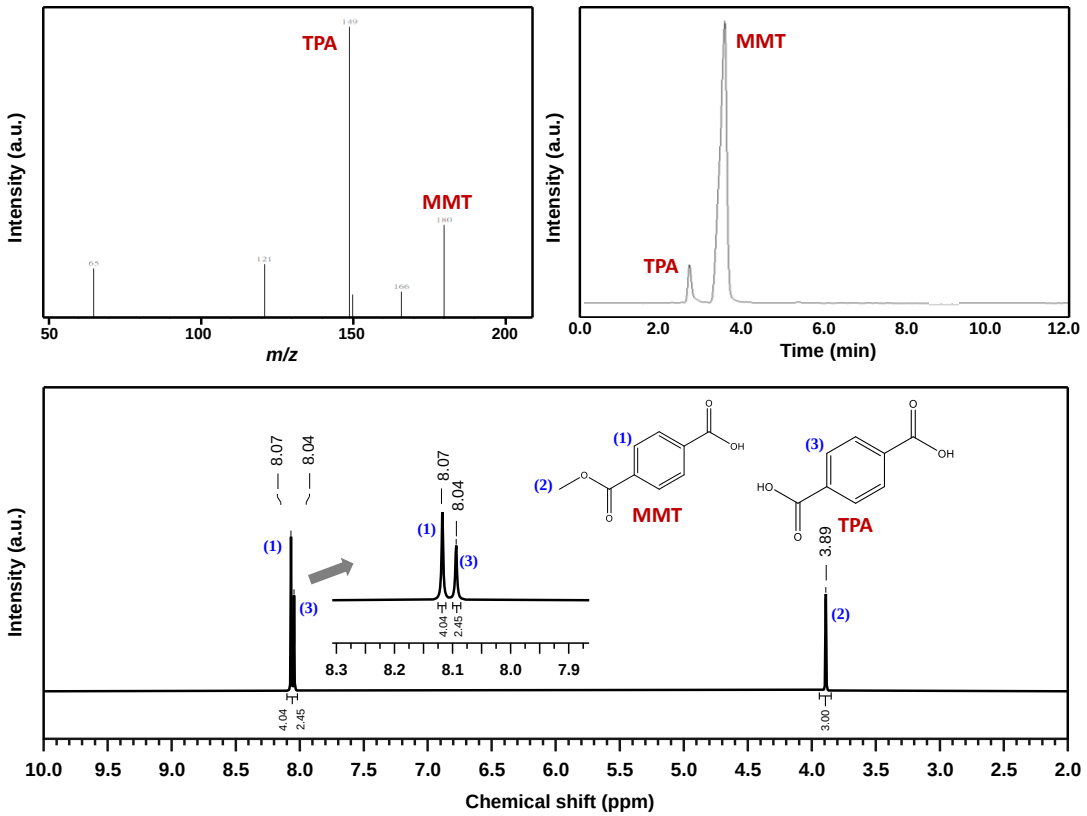

Fig. S3. (a) Fragmentation pattern by EI-MS, (b) HPLC chromatogram, and (c) ^{1}H NMR spectrum of a mixed sample of solid by-products

Fig. S2(a) presents the fragmentation pattern by EI-MS analysis. It can be clearly seen that the determinative peak appears at *m/z* = 194 amu, which is equal to the molecular weight of DMT, and no extrinsic peaks of smaller fragments were found. The result suggests that the obtained monomer is DMT. The sample was analysed by HPLC equipped with a UV detector set at 254 nm and RP C_{18} column. A methanol:water solution (with a volume ratio of 70:30) were applied as a mobile phase at a flow rate of 0.7 mL/min. A single clear and symmetric peak (t_R = 10.89 min) can be found in the HPLC chromatogram (Fig. S2(b)). ^{1}H NMR ($CDCl_3$, 400 MHz) spectrum of the product shows two distinct signals at 8.03 (s, 4H) and 3.88 (s, 6H) (Fig. S2(c)) which can be assigned to four aromatic protons in benzene ring and six protons of methoxy groups, respectively. Fig. S2(d) illustrates measured IR spectrum of the product. The IR spectrum indicates a pure DMT structure. The absorptions at 3000-2800, 1720, 1107 cm^{-1} can be assigned to C-H, C=O and C-O stretching vibration, respectively. The results agree well with the typical characteristic peaks of DMT that are previously reported elsewhere.[1]

Fig. S3 shows the characterization results for a by-product solid sample obtained after post-treatment steps described in Fig. S1. It is expected that the sample comprised of TPA and MMT. In the EI-MS analysis (Fig. S3(a)), two characteristic peaks are measured at 166 and 180 amu, which are corresponding to the molecular weights of TPA and MMT, respectively. The HPLC measurement was repeated for the sample and corresponding chromatograms is shown in Fig. S3(b). Obvious two compounds eluted earlier than DMT, which account for TPA (t_R = 2.65 min) and MMT (t_R = 3.34 min), were detected. ^{1}H NMR (DMSO-d_6, 400 MHz) spectrum of the solid sample exhibit three peaks at δ = 3.89, 8.04 and 8.07 (Fig. S3(c)). The distinctive chemical shifts of aromatic protons in TPA and MMT appeared as two peaks at 8.04 and 8.07. A single lone peak at 3.89 is accountable for the methoxy group of monomethyl terephthalate.[2]

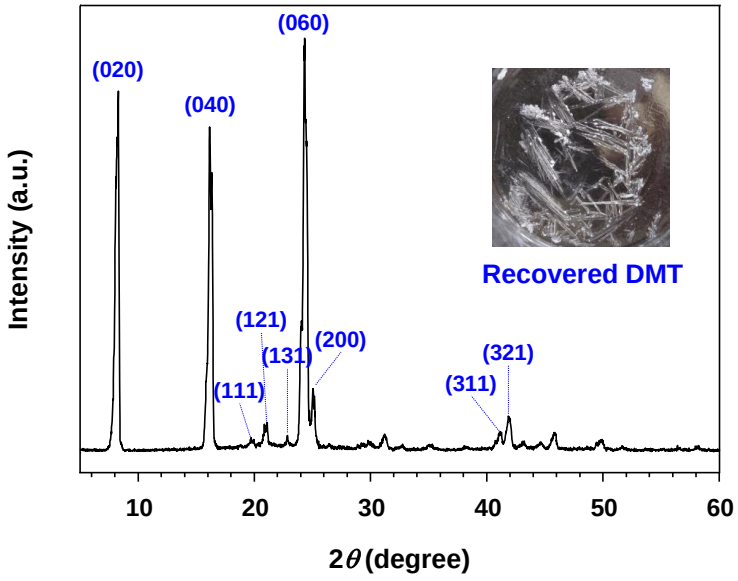

Fig. S4. XRD pattern of DMT product collected by crystallization in cold water (4°C)

Due to the limited solubility of DMT in various organic solvents, crystallization and

recrystallization are the most favoured purification and recovering techniques to produce pure DMT in industrial applications.[3] A slow crystallization of DMT can be observed when an excessive amount of water was mixed with the liquid filtrate of reaction product and stored in a cold refrigerator. Needle-like crystals are completely isolated and applied to a XRD measurement. Fig. S4 shows the XRD pattern of the purified solid sample. All identified peaks belong to the closest packed planes in orthorhombic lattice of DMT.

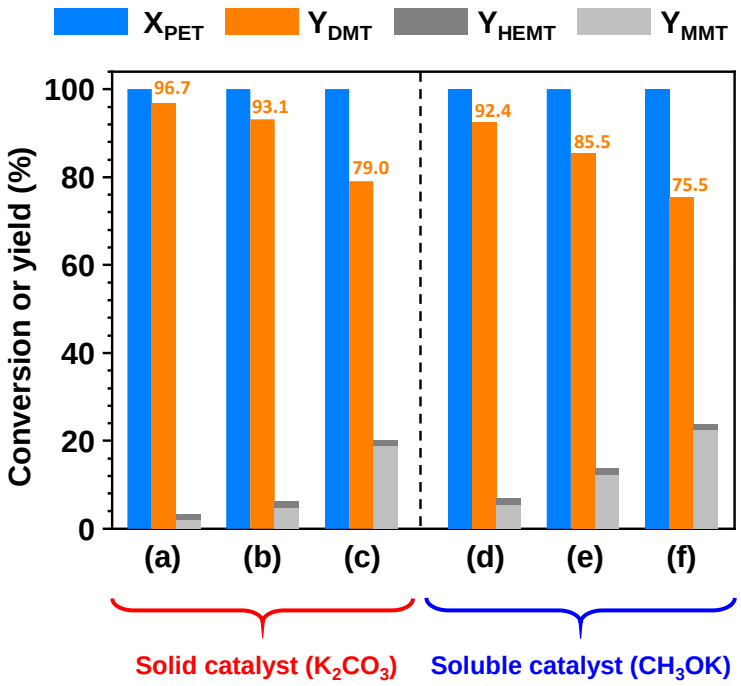

Fig. S5. Effect of initial moisture content on the methanolysis of PET at 25 °C for 24 h in the presence of K_2CO_3 and CH_3OK. The initial molar ratios of water to PET repeating unit were 0.02 for (a) and (d), 0.4 for (b) and (e), and 0.9 for (c) and (f), respectively. The molar ratios of catalyst, methanol, and DCM to PET repeating unit were set to be 0.2, 50, and 50, respectively.

Fig. S5 compares the effects of initial molar amount of water on the catalytic activities of K_2CO_3 and CH_3OK. It is evident that the selectivity of DMT significantly decreases with an increase of water amount in the catalytic solution. A large amount of initial moisture accelerates the formation of MMT while the yields of the other by-product (HEMT) remain almost unchanged for both reaction systems. The reaction system catalysed by solid K_2CO_3 shows a less sensitivity to the initial moisture amount in a reaction mixture when the product distributions for both reaction systems under the identical conditions are compared.

Fig. S6 displays XRD patterns for the remaining part of PET during the solvent-aided catalytic methanolysis. Opaque PET granular particles, expected to comprise mixed phases of amorphous and crystalline polymer chains, are applied for the test. A large fraction of the unreacted PET is left in the reaction solution during the catalytic methanolysis at 25°C for 24 h while the other waste PET samples are fully decomposed. The characteristic peaks for crystalline phase start to appear in the XRD pattern of remaining PET powder. The result

explains that the persistent decomposition behaviour is mainly due to a relatively high composition of crystalline phase in the PET sample.

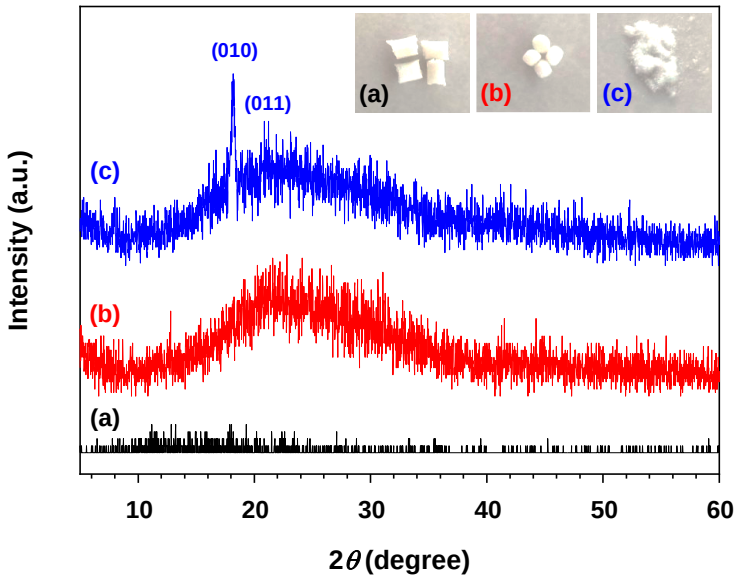

Fig. S6. XRD patterns of solid PET residue recovered after catalytic methanolysis of semicrystalline PET granular particles for (a) 0 h, (b) 12 h, and 24 h.

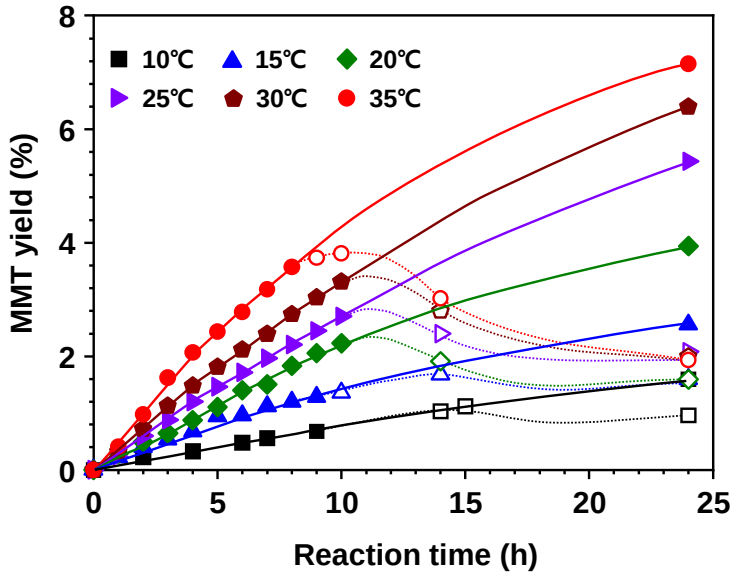

Fig. S7. Kinetic and thermodynamic behaviours of MMT produced from the hydrolysis of DMT. The molar ratios of catalyst, water, methanol, and DCM to DMT were adjusted to be 0.2, 0.4, 50, and 50, respectively. Closed symbols indicate total MMT yields in the solution while open symbols correspond to the soluble DMT yield in the solution.

Fig. S7 shows kinetic and thermodynamic behaviours of MMT that are produced from hydrolysis of DMT in the absence of EG. Compared to the case of EG presence (presented in Fig. 9 in the main manuscript), the overall rate of hydrolysis was increased by the rate of HEMT production. A large amount of cation exchanged MMT, which is the only decomposed product in the reaction, concentrated in the solution till the reaction proceeds for 8 h. At this thermodynamically unstable condition, a large amount of K-MMT are supersaturated in the reaction solution. However, a continuous hydrolysis for a long reaction time causes the excess solute to eventually precipitate. The absence of EG does not induce the formation of HEMT and the solubility of K-MMT in the reaction solution was significantly lowered. Although the hydrolytic conversion of DMT and the phase transition of K-MMT occurs simultaneously, the final yields of K-MMT were rarely influenced by the concentration in either solution or solid precipitate.

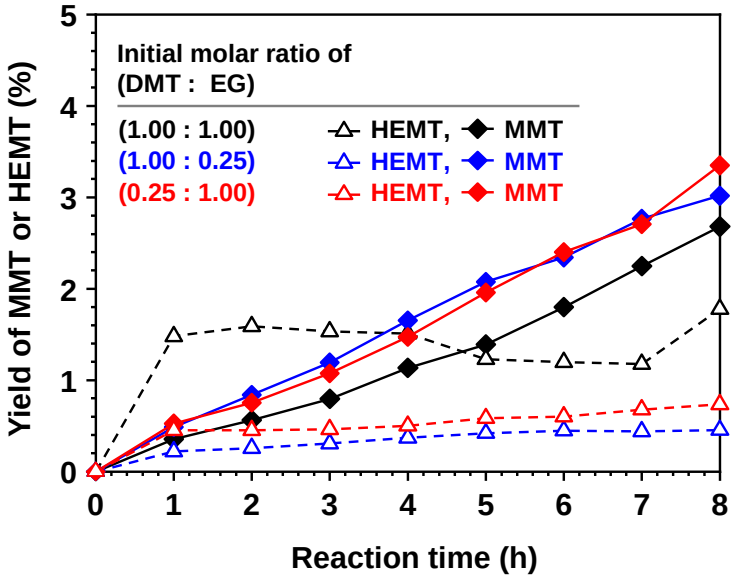

Fig. S8. Observation of kinetic behaviours of DMT decomposition by limiting one of initial concentrations of DMT or EG. The molar ratios of catalyst, water, EG, methanol, and DCM to DMT for the base case (DMT:EG = 1:1) was 0.2, 0.4, 1.0, 50, and 50, respectively.

Fig. S8 shows the dependence of the initial molar amount of reactant on the final yields of MMT and HEMT in the reaction system of DMT decomposition. A decrease in molar amount of reactants reduces an equilibrium concentration of HEMT. However, an accumulated amount of MMT was observed to increase. It is notable that both reactions apparently exhibit a competitive parallel reaction.

Fig. S9 show the effect of reaction temperature on the solvent-assisted PET methanolysis. It is obvious that the PET particles are more rapidly decomposed into monomers with an increased reaction temperature. However, the final yield of DMT was observed to be much lower at a high reaction temperature. It is ascribed to the pre-dominant hydrolysis of DMT which can be more effectively promoted by transesterification catalysts. Notably, equilibrium

concentration of HEMT was not dependent on the reaction temperature.

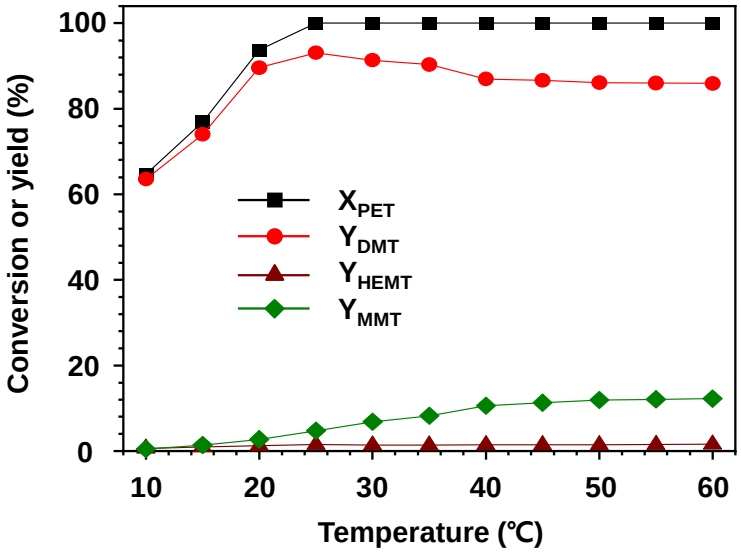

Fig. S9. Effect of reaction temperature on the PET methanolysis. The reaction at 10-35℃ performed for 24 h. For the reaction performed at a high temperature of 40℃ or above, the final reaction time was adjusted to the onset point that a complete decomposition of PET is observed. The molar ratios of catalyst, water, methanol, and DCM to PET repeating unit were adjusted to be 0.2, 0.4, 50, and 50, respectively.

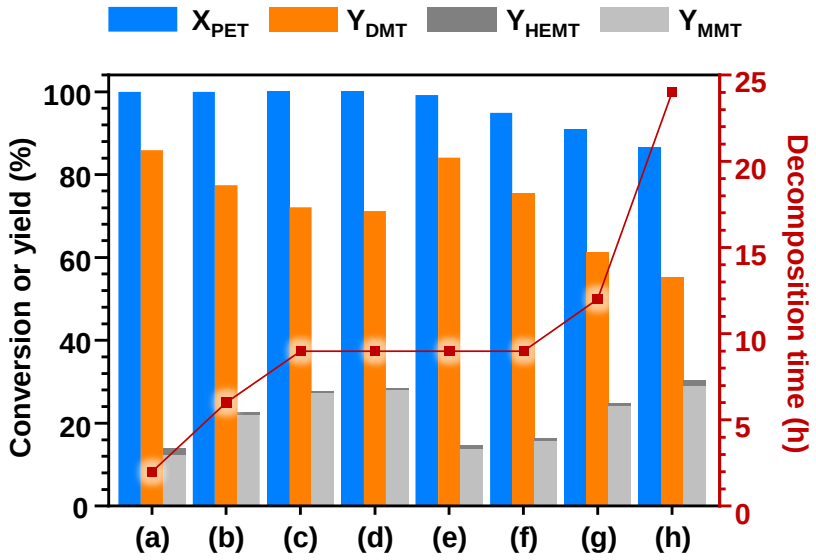

Fig. S10. Effect of co-solvent on the PET methanolysis at 60℃. As a co-solvent, (a) DCM, (b) chlorobenzene, (c) methoxy benzene, (d) toluene, (e) THF, (f) dioxane, (g) acetonitrile, or (h) acetone was applied to the methanolysis. The molar ratios of catalyst, water, methanol, and co-solvent to PET repeating unit were adjusted to be 0.2, 0.4, 50, and 50, respectively.

Several aprotic polar solvents were used as a co-solvent to explore a new combination for the efficient catalytic methanolysis at 60°C. Few simple examples are presented in Fig. S10. Although the current investigations were not successful to find a highly selective or an optimized compositions of solvents, it was ascertained that the combinations of multiple cosolvents with different functionalities can be applied for an efficient conversion of PET into DMT at a low reaction temperature.

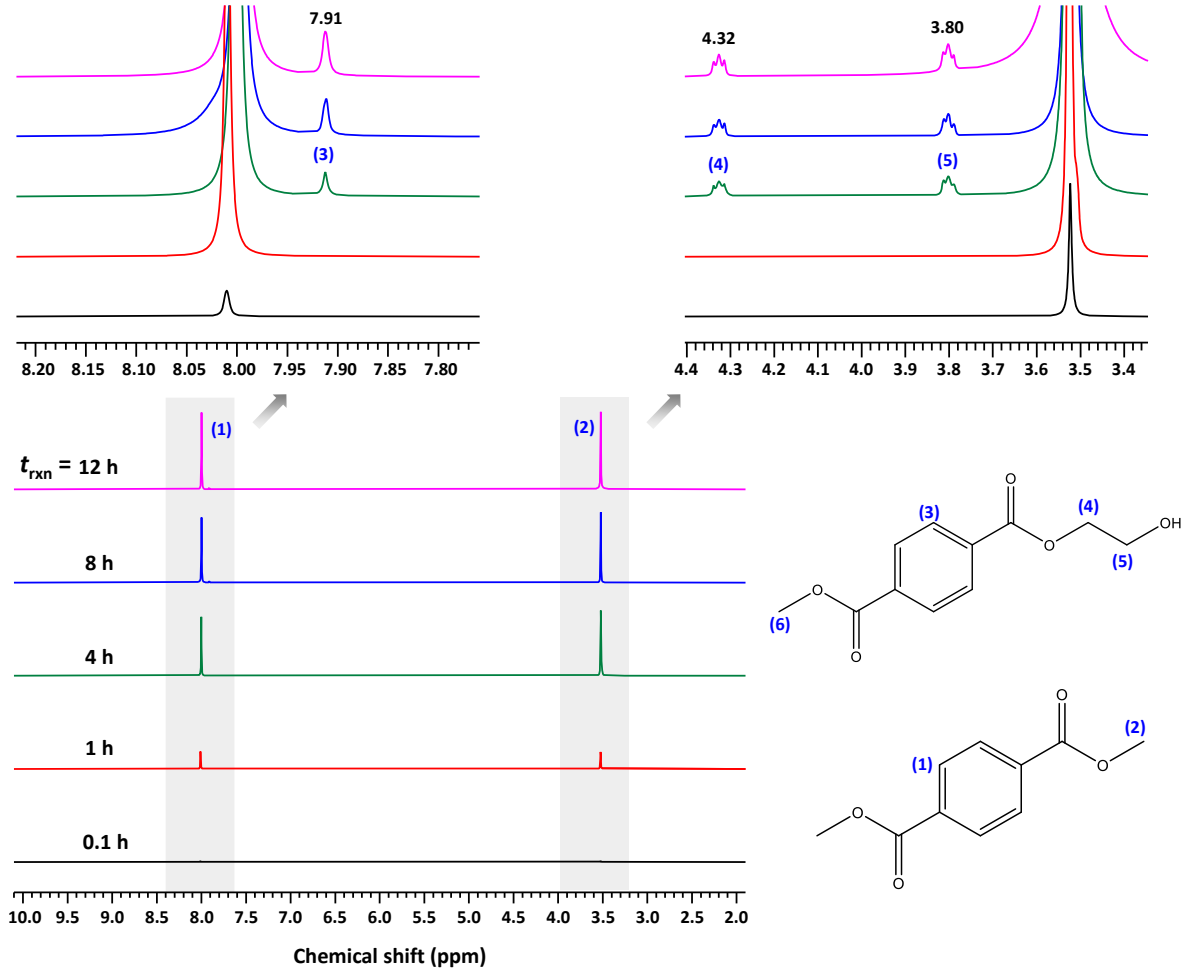

Fig. S11. Kinetic ^{1}H-NMR analysis for the solvent-aided catalytic methanolysis system. The molar ratios of catalyst, CD_3OD, and CD_2Cl_2 to PET were adjusted to be 0.2, 50, and 50, respectively.

Fig. S11 illustrates the time-dependent ^{1}H NMR spectra for the methanolysis reaction at the same reaction condition with the base case. The reaction system was carried out in a closed NMR tube attached to a crossed magnetic stirring bar and immersed in a constant temperature (25°C) water bath. During the reaction, the NMR tube was continuously spinning by a magnetic stirrer. At a desired reaction time, the NMR tube was transferred to an NMR spectrometer to measure the spectrum data and returned back to the reaction system right away. In this kinetic analysis, extrinsic or unexpected peaks were not found. The strong peaks accounting for aromatic protons in benzene ring and protons in methoxy group of DMT appear at 3.52 ppm

(s, 6H) and 8.01 ppm (s, 4H). Their intensities are keep increasing while few low intensity peaks, responsible for protons in typical functional groups belong to HEMT, start to appear at 3.80, 4.32 and 7.91 after 4 h. Their absolute peak areas were kept almost constant during the reaction. The kinetic behaviour measured by NMR shows a good agreement with that measured by HPLC, as time-dependent chromatograms are depicted in Fig. S12.

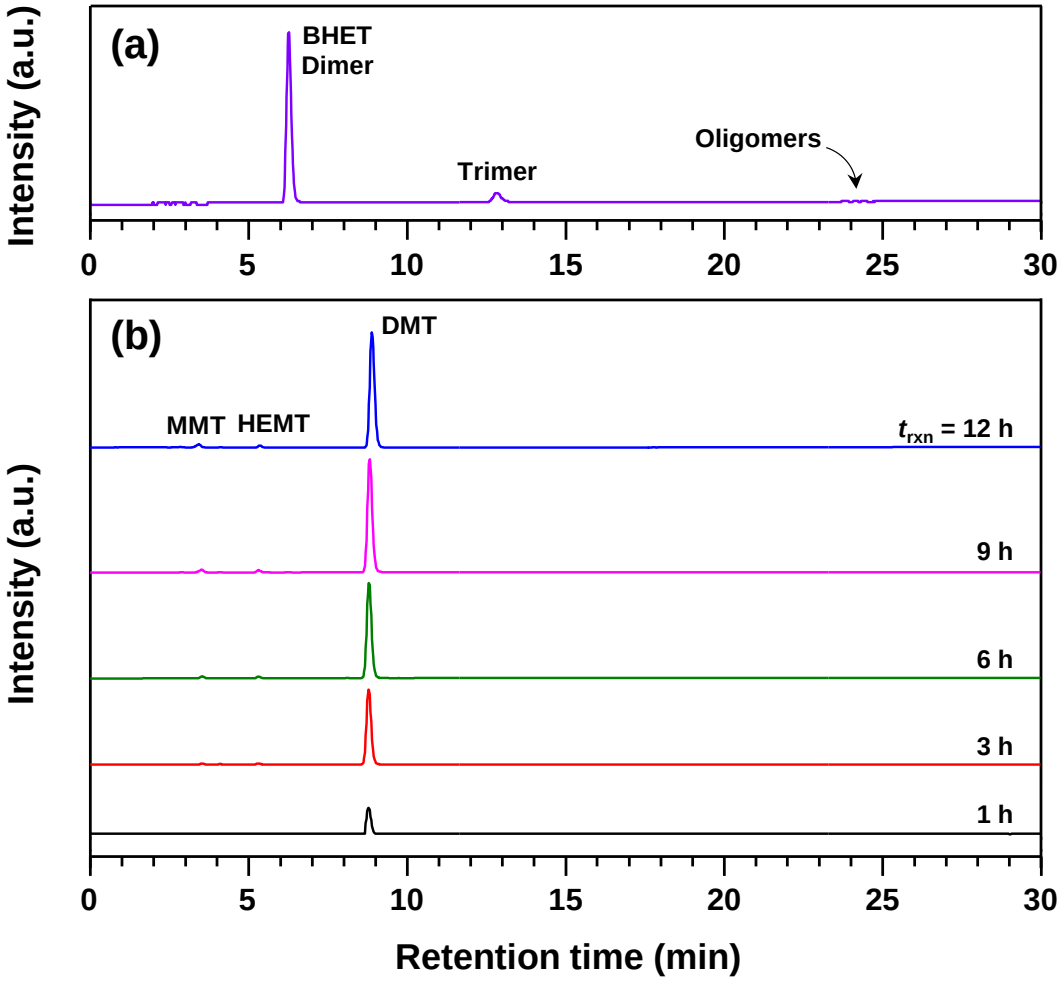

Fig. S12. HPLC chromatograms of (a) thermally decomposed products by glycolysis and (b) the time-dependent measurement of monomer products evolved from solvent-aided catalytic methanolysis. The molar ratios of catalyst, water, methanol, and DCM to PET repeating unit were adjusted to be 0.2, 0.4, 50, and 50, respectively.

Fig. S13 shows the time-dependent FT-IR spectra of PET flake during the catalytic methanolysis reaction. It is obvious that the relative peak intensities for functional groups including ester bond gradually decrease along the reaction time. And no additional extrinsic peak appears in those spectra. It is evident that the overall degradation of the polymer is steady and slow. The result supports the hypothesis of gradual PET degradation by end-group scission during the catalytic methanolysis.

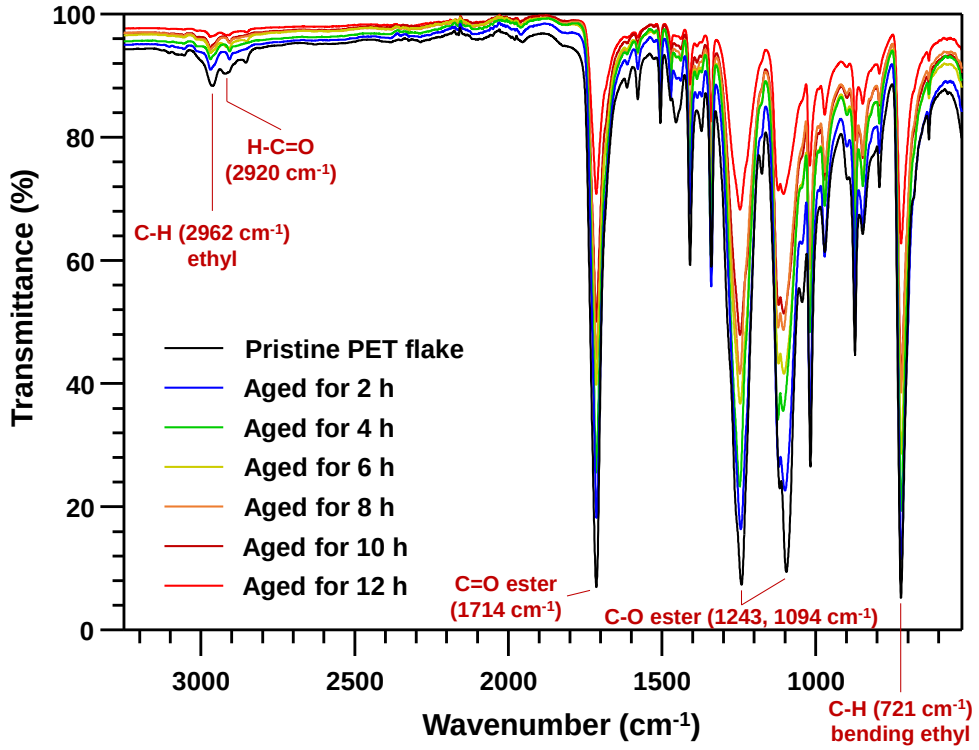

Fig. S13. FT-IR spectra of PET flakes during the catalytic methanolysis. The molar ratios of catalyst, water, methanol, and DCM to PET repeating unit were adjusted to be 0.2, 0.4, 50, and 50, respectively.

REFERENCES

1. M. N. Siddiqui, H. H. Redhwi and D. S. Achilias, *Journal of Analytical and Applied Pyrolysis*, 2012, **98**, 214-220.
2. S. Mishra and A. S. Goje, *Polymer international*, 2003, **52**, 337-342.
3. Y. Li, J. Qi, B. Fan, J. Tang, X. Lin and Q. Li, *Journal of Molecular Liquids*, 2020, **297**, 111546.